Hydrogen spectral lines with the inclusion of dense-plasma effects

S. Günter
Fachbereich Physik, Universität Rostock, Universitätsplatz 3, O-2500 Rostock, Germany

L. Hitzschke
Zentralinstitut für Elektronenphysik, Hausvogteiplatz 5-7, O-1086 Berlin, Germany

G. Röpke
Fachbereich Physik, Universität Rostock, Universitätsplatz 3, O-2500 Rostock, Germany
(Received 21 August 1990; revised manuscript received 9 April 1991)

Line profiles for hydrogen including the case of dense plasmas are investigated on the basis of a many-particle approach. Using a Green's-function technique, electron contributions to the shift and broadening from both separate-level and interferencelike terms are considered consistently. The theoretical approach to the line profile has been improved by including dynamic screening of collisions, contributions from $\Delta n=0$ transitions, and cross-term contributions not only to the broadening but also to the shift of the line. As an example, the line profile of H_α has been considered. An analysis of details of the second-order approximation with respect to the atom-plasma interaction is given, avoiding the no-quenching and dipole approximations. The effect of dynamic screening for high electron densities is investigated. Deviations from the linear dependence between the electron-shift contribution and the density are expected for H_α for $n_e \geq 2\times 10^{18}$ cm^{-3} at temperatures of about 10 000 K.

PACS number(s): 52.25.Rv, 32.70.Jz

I. INTRODUCTION

Stark broadening of spectral lines provides a valuable tool for investigations in the field of plasma physics. In order to study the connection between the observed line shapes and the microscopic processes within the plasma, in principle, a quantum statistical many-body system has to be considered. In the low-density limit it is sufficient to consider collisions of the atom and a perturbing charged particle [1]. However, with increasing density the concept of a single emitting atom within an environment of perturbers becomes unrealistic. This means that, instead of single-particle effects such as binary collisions, collective degrees of freedom such as plasma oscillations become more important.

Generally, a Green's-function approach seems to be well suited to a rigorous description of these effects. In fact, using the advantages of the diagram technique, it is much easier to find a complete set of contributing terms within a definite frame of approximations. Green's-function approaches have already been used by different authors to describe the Stark broadening of spectral lines [2–7]. Besides investigations based on that technique, an equivalent approach is rooted in a formal application of kinetic theory in connection with a Liouville-operator technique [8–12].

Recently, the concept of a general quantum-statistical theory to the description of thermodynamic, transport, and optical properties in dense plasmas has been accomplished [13,14]. In this way, a many-particle approach to the theory of spectral lines has been developed using the Green's-function concept. As a starting point, the relationship between optical properties and the dielectric function has been chosen [15–17]. A diagram technique has been used to select out the relevant approximations within the perturbative expansion. It has been shown [18] that this Green's-function approach corresponds, in principle, to the kinetic-theory approach, and that the semiclassical impact approximation [1] comes out as a special approximation [17]. Furthermore, on the basis of this approach, the shifts and widths of some argon lines have been calculated and compared with experimental results [19]. Moreover, attempts have been made to describe nonlinearity effects with respect to the density dependence of shift and broadening of lines in dense plasmas [19]. So, a general quantum-statistical approach to spectral-line shapes is available. However, in evaluating spectral-line profiles, overlapping lines have been excluded by neglecting degenerate or close-lying energy levels within the unperturbed atomic system [17,19,20].

The aim of the present paper is threefold. First, improving on previous work [17,19,20], overlapping lines were included in the Green's-function approach. Therefore the self-energy and vertex contributions to the electron shift and broadening were reconsidered, as described in Sec. II. Thereby an additional contribution to the line shift, the vertex contribution, was found for overlapping lines. Second, based on the final expressions of Sec. II and further approximations which are discussed in Sec. III, line-profile calculations, in particular for H_α, were performed. In Sec. IV a detailed analysis of the corresponding results is given. Finally, Sec. V is devoted to the question of whether or not effects of dynamic screening of the electron-atom interaction with increasing density are important. Such effects have been discussed recently for some Cs I lines [21] and have been confirmed experimentally [22].

II. THEORY

Based on a Green's-function technique, a systematic approach to spectral-line shapes in dense plasmas has been developed (for a short introduction see Refs. [14–20] as well as Appendix A). In principle, this Green's-function approach is able to describe the optical properties of plasmas over the full density-temperature range. Most descriptions of spectral lines in plasmas are based on a quasistatic approximation for the ions and a collisional formulation for the electrons. In fact, at least for the small plasma parameters considered here, it is possible to decouple the ion and electron subsystems by treating the ion-electron correlation within a microfield distribution, where the ion field is shielded by electrons in the Debye-Hückel form [23].

The objective of this paper is to investigate the electron contributions to hydrogen spectral lines, reconsidering the interaction between the bound and the perturbing electrons in a systematic manner. The electron contribution to the line shape can be obtained from the imaginary part of the corresponding polarization function [14–20] (see Appendix A), whereas the line-shape function reads

$$I(\omega)=\frac{1}{\pi}\int_0^\infty d\beta\, W(\beta)\,\mathrm{Im}\sum_{i',f',i'',f''}\langle i''|\mathbf{r}|f'\rangle\langle f''|\mathbf{r}|i'\rangle \times\langle i'|\langle f'|[\omega-H_i^0(\beta)+H_f^0(\beta)+\mathrm{Re}(\Sigma_f-\Sigma_i)+i\,\mathrm{Im}(\Sigma_i+\Sigma_f)+i\Gamma_{if}^V]^{-1}|f''\rangle|i''\rangle\ , \tag{2.1}$$

with

$$H(\beta)=H^{(0)}+C(\beta)\ . \tag{2.2}$$

Because it is more convenient to treat the problem of energy-level splitting caused by the ion microfield within parabolic coordinates, the states i', i'', f', and f'' in Eq. (2.1) have to be considered as the degenerate initial and final states, respectively, within parabolic coordinates. In addition, in Eq. (2.1) the "line-space" notation according to Baranger [24] was introduced, allowing the Hamiltonians H_i and H_f to act only within the space of initial and final states. $W(\beta)$ stands for the microfield distribution function, where $\beta=E/E_0$ denotes the normalized and E_0 the Holtsmark (normal) field strength. In this paper the microfield distribution according to Hooper [25] has been chosen. Furthermore, the Stark splitting of the degenerate energy levels is defined by the corresponding operators C [26] while $\langle i|\mathbf{r}|f\rangle$ has to be identified with the dipole matrix element for the transition between the states i and f.

The level shift and broadening results from the self-energy operator Σ, whereas the operator of the vertex contribution Γ^V generates the upper-lower interference term. The self-energy and the interferencelike terms follow from the interaction between the radiating atom and the plasma environment. Therefore, in order to determine Σ and Γ^V it is necessary to deal with a many-particle problem. The latter can be treated in the frame of a perturbative expansion. Using the Green's-function approach, it is possible to carry out this perturbative expansion in a very systematic manner. Relevant parameters for such a perturbative approach are the perturber density and the atom-perturber interaction. Due to the fact that our main concern is directed to weakly nonideal plasmas, it is reasonable to restrict all of the following theory to modifications in the line shape which are linear in the density of the perturbing electrons. However, due to the collective degrees of freedom, the effective electron-atom interaction becomes a dynamic one. Therefore, in calculating Σ and Γ^V, as the simplest approximation, a first-order Born approximation with respect to the dynamically screened electron-atom interaction has been considered. Of course, the developed Green's-function approximation is more general and is not restricted to the introduced simple approximations.

Analogous to Ref. [17], Σ and Γ^V were calculated at the same level of approximation. The final expressions in matrix representation read

$$\langle i'|\Sigma|i''\rangle=-\frac{1}{e^2}\int\frac{1}{(2\pi)^3}d\mathbf{q}\,V(q)\frac{1}{\pi}\int_{-\infty}^{+\infty}d\omega\,\mathrm{Im}\epsilon^{-1}(\mathbf{q},\omega+i\delta)[1+n_B(\omega)] \times\sum_\alpha\frac{1}{E_i^0-E_\alpha^0-(\omega+i\delta)}M_{i'\alpha}^{(0)}(\mathbf{q})[M_{i''\alpha}^{(0)}(\mathbf{q})]^*\ , \tag{2.3}$$

with $n_B(\omega)=(e^{\beta\omega}-1)^{-1}$, $\beta=1/k_BT$, and the Coulomb potential $V(q)=4\pi e^2/q^2$. Thus within the frame of our approximations it is sufficient to take the dielectric function of the electron gas $\epsilon(\mathbf{q},z)$ in random-phase approximation (RPA):

$$\epsilon(\mathbf{q},z)=1-2\int\frac{1}{(2\pi)^3}d\mathbf{p}\,V(q)\frac{f_e(E_\mathbf{p})-f_e(E_{\mathbf{p}+\mathbf{q}})}{E_\mathbf{p}-E_{\mathbf{p}+\mathbf{q}}-z}\ . \tag{2.4}$$

The expression

$$M^{(0)}_{n\alpha}(\mathbf{q})=ie\int\frac{1}{(2\pi)^3}d\mathbf{p}\,\Psi^*_n(\mathbf{p})[\Psi_\alpha(\mathbf{p})-\Psi_\alpha(\mathbf{p}+\mathbf{q})] \tag{2.5}$$

denotes the isolated vertex function, where Ψ is the wave function of the isolated atom. The upper-lower interference term reads

$$\langle i'|\langle f'|\Gamma^V|f''\rangle|i''\rangle=-\frac{2}{e^2}\int\frac{1}{(2\pi)^3}d\mathbf{q}\,V(q)\sum_{n_1,n_1',n_2,n_2'}M^{(0)}_{i''n_1}(\mathbf{q})M^{(0)}_{n_2'f'}(-\mathbf{q})M^{(0)}_{n_1'n_2}\left[\frac{\omega^{(0)}_{if}}{c}\right]\Big/M^0_{i''f'}\left[\frac{\omega^{(0)}_{if}}{c}\right]$$
$$\times\int_{-\infty}^{+\infty}\frac{L_{i'f'i''f''}}{L_{n_1n_2n_1'n_2'}}[1+n_B(\omega)]\mathrm{Im}\epsilon^{-1}(\mathbf{q},\omega+i\delta)d\omega\ , \tag{2.6}$$

with

$$L_{i'f'i''f''}=\langle i'|\langle f'|\omega+H^0_f-H^0_i+\mathrm{Re}(\Sigma_f-\Sigma_i)+i\,\mathrm{Im}(\Sigma_i+\Sigma_f)|f''\rangle|i''\rangle\ ,$$

where $\omega^{(0)}_{if}$ is the unperturbed transition frequency for transitions between the energy level i and f. (For more details see Appendix A.)

The self-energy and the vertex contributions according to Eqs. (2.3) and (2.6) have to be considered as a generalization of those for isolated lines [see Eq. (3.16) and (3.17) of Ref. [17]]. In contrast to the latter, however, the generalized vertex contributions given by Eq. (2.6) lead not only to the well-known contribution to the broadening of the line, but also to an additional term, the vertex contribution to the line shift.

The first-order Born approximation introduced above is restricted to weak electron-atom collisions. The treatment of strong electron-atom collisions has to avoid a perturbative expansion with respect to the interaction. However, in contrast to the case of weak collisions, collective effects such as screening lose their importance, as is well known from the evaluation of transport properties. Using the Green's-function concept again, and assuming the electron-atom interaction as an elastic-scattering process, the connection between self-energy contributions to the level shift and broadening and the phase shifts δ_l can be derived ending up with

$$\Delta_n+i\Gamma_n=\frac{-2\pi}{m_e}\int\frac{1}{(2\pi)^3}d\mathbf{p}\,f_e(E_p)\frac{1}{p}$$
$$\times\sum_l(2l+1)e^{i\delta_l(E_p)}\sin\delta_l(E_p)\ , \tag{2.7}$$

which corresponds to Baranger's result [24]. (See also Appendix B for details.)

III. APPROXIMATIONS

In order to calculate hydrogen spectral lines, starting from Eqs. (2.1)–(2.6) and considering only the low-density limit, it is useful to introduce further approximations.

First, the Fermi distribution of the electrons may be replaced by the Boltzmann distribution

$$f_e(E_p)\approx\tfrac{1}{2}n_e\left[\frac{2\pi}{m_ek_BT}\right]^{3/2}\exp(-p^2/2m_ek_BT)\ , \tag{3.1}$$

where n_e and m_e are the electron density and mass, respectively. Quantum effects that are connected with the use of a Fermi distribution are not of importance in the density region ($n_e<10^{19}$ cm^{-3}) considered here. However, further quantum effects, as given by $\mathrm{Im}\epsilon^{-1}$, are of more importance in this region. They lead to a convergent behavior of the integrals for shift and broadening according to Eqs. (2.3) and (2.6). Furthermore, the expression

$$\mathrm{Im}\epsilon^{-1}(\mathbf{q},\omega)=-\frac{\mathrm{Im}\epsilon(\mathbf{q},\omega)}{[\mathrm{Re}\epsilon(\mathbf{q},\omega)]^2+[\mathrm{Im}\epsilon(\mathbf{q},\omega)]^2}\ , \tag{3.2}$$

occurring in (2.3) and (2.6), can be simplified for hydrogen line profile calculations.

The main contributions to the shift and broadening according to (2.3) and (2.6) are to be expected at the unperturbed transition frequencies $\omega\approx\omega^{(0)}_{i\alpha}=E^{(0)}_i-E^{(0)}_\alpha$. Therefore, as long as the plasma frequency $\omega_{\mathrm{pl}}=(4\pi n_ee^2/m_e)^{1/2}$ is small compared to $\omega^{(0)}_{i\alpha}$, for calculations of contributions from virtual transitions between states with different principal quantum numbers ($\Delta n\neq0$ contributions) using the RPA dielectric function, the approximation

$$\mathrm{Im}\epsilon^{-1}(\mathbf{q},\omega)\approx-\mathrm{Im}\epsilon(\mathbf{q},\omega) \tag{3.3}$$

holds.

For the $\Delta n=0$ contributions a Debye screened electron-atom interaction may be applied, using

$$\mathrm{Im}\epsilon^{-1}(\mathbf{q},\omega)\approx-\frac{\mathrm{Im}\epsilon(\mathbf{q},\omega)}{(1+\kappa_D^2/q^2)^2} \tag{3.4}$$

if $\omega^{(0)}_{i\alpha}\ll\omega_{\mathrm{pl}}$ is fulfilled. Here κ_D denotes the inverse Debye radius $\kappa_D=(4\pi n_ee^2/k_BT)^{1/2}$.

Both approximations work well if only the electron densities are small ($n_e\leq10^{18}$ cm^{-3}). However, with increasing densities, the energy difference between the perturbing states may become comparable to the electron plasma frequency ω_{pl}. Thus, for such a situation the use of the approximations (3.3) and (3.4) is no longer valid, and one has to take the full expression (3.2). This problem will be discussed in detail in Sec. V. As usual, in calculating the electron contributions to shift and broadening, the level splitting due to the ion microfield has been neglected. As with the problem of screening, this can be

done if the ion density is small (see Sec. V).

Finally, for the evaluation of the matrix elements in Eq. (2.5), the multipole expansion was avoided, using instead the more general expansion of $e^{i\mathbf{q}\cdot\mathbf{r}}$ into spherical harmonics $Y_{lm}(\theta,\phi)$,

$$e^{i\mathbf{q}\cdot\mathbf{r}}=4\pi\sum_{l=0}^{\infty}\sum_{m=-l}^{l} i^l j_l(qr)Y_{lm}^*(\Omega_q)Y_{lm}(\Omega_r)\ , \qquad (3.5)$$

where j_l stands for the Bessel function. Considering weak collisions one can restrict to only $l=0$ and 1 contributions in Eq. (3.5). That corresponds to an inclusion of multipole contributions up to dipolelike terms.

In order to investigate the contributions of strong collisions, the phase shifts occurring in Eq. (2.7) have to be evaluated. An adequate treatment of strong collisions can be formulated on the strength of close-coupling equations [27]. For simplicity, here a partial summation of the perturbative expansion has been used. In a first approximation this leads to a static polarization potential for the electron-atom interaction (see Refs. [28,29] and Appendix B).

In order to get an idea of the shift and broadening behavior with respect to strong collisions, the shift of the central L_α component corresponding to the $001\rightarrow000$ transition (in parabolic quantum numbers) has been evaluated. In Fig. 1 the results of the phase-shift calculations are compared with those of the Born approximation [Eq. (2.3)] in an adiabatic approximation. In addition, a comparison is made with shifts which are obtained after carrying out the transition to the semiclassical approach in Eq. (2.3) (compare, e.g., Ref. [17]) and using the dipole approximation in calculating $M_{n\alpha}^{(0)}(\mathbf{q})$. It is obvious from Fig. 1 that the treatment of strong collisions by phase-shift calculations leads to an improvement of the first-order Born approximation. But it is to be seen also that the contributions of strong collisions are further overestimated as the result of the introduced adiabatic approximation.

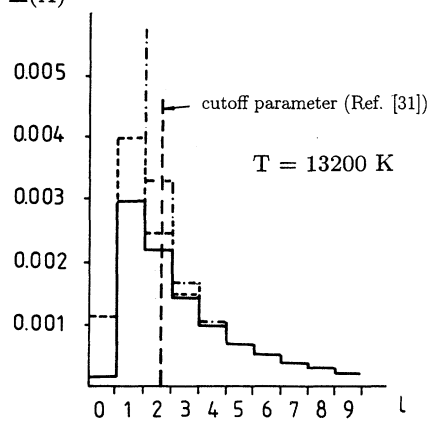

FIG. 1. Electron shift contributions to the 001 state (parabolic coordinates) as a function of the angular momentum numbers l. ——, results using Eq. (2.7) and the phase shifts based on Eq. (B6); — — —, results from treating the perturbing electrons in agreement with Eq. (2.3) within adiabatic approximation; —·—·—·, results from treating the perturbing electrons classically within adiabatic approximation [the corresponding q integrals in Eq. (2.3) are performed within the limits $q=[\bar{p}/(l+1),\bar{p}/l]$ with $\bar{p}=\sqrt{3k_BT/m_e}$].

As a very simple way to avoid the overestimation occurring in the Born approximation for small l (strong collisions), the introduction of a cutoff procedure has proved feasible. Here the procedure suggested by Griem [31] will be applied: The q integrals in Eqs. (2.3) and (2.6) will be cut at a maximal value $q_{\max}=1/\rho_{\min}$, where $\rho_{\min}$ is to be calculated in agreement with Ref. [31]. The strong-collision contributions to the broadening are estimated within a Lorentz-Weisskopf approximation; they introduce an additional shift of about 20% of that due to weak-collision contributions.

IV. RESULTS AND DISCUSSION OF THE LINE-SHAPE CALCULATIONS FOR LOW-DENSITY PLASMAS

In order to test the theory given here, the profile of the H_α line for hydrogen was calculated and has been compared with experimental results. After evaluating Eq. (2.1), for H_α the profile of Fig. 2 resulted. An excellent agreement between the unified theory calculations [32] and our theory can be stated. At this point it is important to recall that the latter should be considered as a correct low-density result within the framework of the static-ion model [33,34]. Therefore this agreement may be regarded as an indication that the treatment of strong collisions given in Sec. III can be justified.

On the other hand, a remarkable difference between our results and that of Ref. [1] has been obtained. The reason for this discrepancy is the inadmissible approximation in determining the vertex contributions. In Ref. [1], in fact, contributions to the vertex term resulting from the degeneracy of the corresponding atomic levels were not taken into account. To prove the effect of this

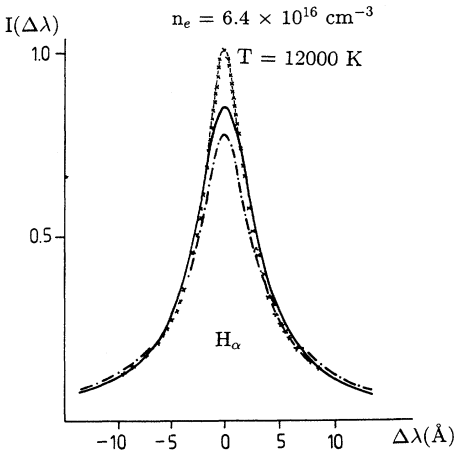

FIG. 2. Calculated H_α-line profiles compared with experiment. ——, experiment (Ref. [36]); ×××, unified theory (Ref. [32]); —·—·—·, Griem (Ref. [1]); — — —, this paper.

approximation on the line shape, the entire profile has been recalculated neglecting the degeneracy with respect to vertex corrections, which corresponds to a setting of $n_1=n_{1'}=i'=i''$, and $n_2=n_{2'}=f'=f''$ in Eq. (2.6),

$$\Gamma^V_{i'f'}=\frac{-2}{e^2}\int\frac{1}{(2\pi)^3}d\mathbf{q}\,M^{(0)}_{f'f'}(-\mathbf{q})M^{(0)}_{i'i'}(\mathbf{q})V(q)\times\int_{-\infty}^{+\infty}d\omega[1+n_B(\omega)]\times\mathrm{Im}\epsilon^{-1}(\mathbf{q},\omega+i\delta)\delta(\omega)\ . \tag{4.1}$$

The resulting profile (Fig. 3) then nearly coincides with that of Ref. [1]. Our theory, of course, is not restricted to a no-quenching approximation (i.e., contributions from nonradiative transitions between states of different principal quantum numbers are considered). Furthermore, from Eq. (2.3) it follows that the correct quantum-mechanical treatment leads to both shift and broadening contributions for virtual transitions with $\Delta n=0$.

In agreement with Eq. (2.1), the full profile of the H_α line can be found after a weighted superposition of all shifted and broadened components of the line. Therefore, in principle, the line shift is obtained only after this superposition procedure. A weighted summing of all shift components as proposed in Ref. [31] is an approximation. Furthermore, the vertex contributions as given by Eq. (2.6) should not be neglected; for H_α it amounts to about 20% of the shift.

Table I shows a comparison of different calculation procedures for the electron contributions to the H_α-line shift. The result of the correct superposition is compared with that of a weighted summing procedure. Values of Ref. [35] have been included. Although the coincidence of the line shift by Griem [35] with the results of the weighted summing procedure of the self-energy contributions should be viewed as fortunate, our self-energy contributions to the shift agree very well with the results there. Nevertheless, it is obvious from Table I that the use of a weighted sum is problematic. The agreement between the calculated shifts of Ref. [35] and those of this paper has been reached only by the inclusion of the vertex contributions.

As discussed in Sec. III the multipole expansion was not used. Instead a decomposition of $M^{(0)}_{n\alpha}(\mathbf{q})$ into spherical harmonics [see Eq. (3.5)] has been applied. Note that the first ($l=0$) term of this series does not occur in a multipole expansion. Calculating the matrix elements $M^{(0)}_{n\alpha}(\mathbf{q})$ defined in Eq. (2.5) according to (3.5) one finds that the leading contribution of the second ($l=1$) term is connected with the dipole matrix by

$$M^{(0),l=1}_{n\alpha}(\mathbf{q})=M^{(0),\mathrm{dipole}}_{n\alpha}\frac{(1/n+1/\alpha)^{2(n+\alpha)}}{[(1/n+1/\alpha)^2+q^2]^{(n+\alpha)}}\ . \tag{4.2}$$

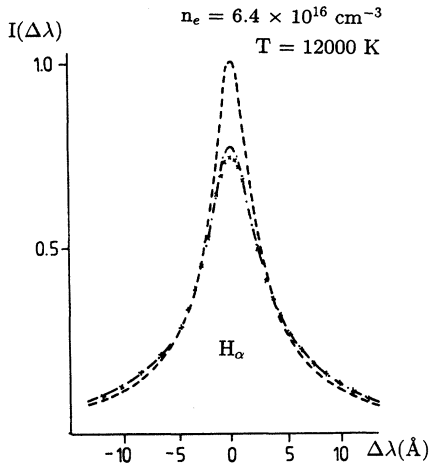

FIG. 3. Calculated H_α-line profiles from different treatments of the interferencelike contributions Γ^V. — — —, as in Fig. 2 based on Eq. (2.6); ×××, as (— — —), but neglecting in Γ^V the degeneracy of the atomic levels; —·—·—·, Griem (Ref. [1]).

It is obvious from Fig. 1 that for small distances between the atom and the perturbing electron, the dipole approximation fails to work. But, as usual, due to the cutoff for strong collisions, errors resulting from the dipole approximation do not influence the final results. This is also true for the higher-order terms in Eq. (3.5) which are small and have been neglected.

For the sake of completeness the profiles for L_α and L_β have been calculated also bearing in mind that the influence of the ion dynamics effects cannot be neglected as before. In fact, their incorporation results in an increase of the L_α half-width by a factor of about 2 and, furthermore, leads to a remarkable reduction of the dip in the center of L_β [37–40], while for H_α the half-width

TABLE I. Electron shift of the H_α line at $\frac{1}{4}$ of the intensity maximum ($n_e=10^{17}$ cm^{-3}, $T=12\,000$ K).

Line shift including vertex corrections to the shift and width (superposition procedure)	0.641 Å
Line shift including vertex corrections to the width only (superposition procedure)	0.625
Line shift without vertex corrections (superposition procedure)	0.781
Line shift without vertex corrections (weighted summing procedure)	0.645
Griem (Ref. [35])	0.645

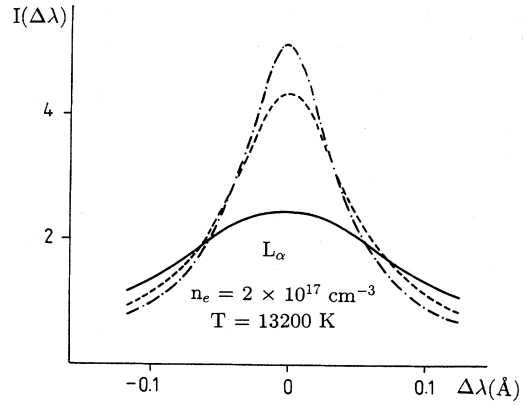

FIG. 4. Results for the L_α-line profile. ——, experiment (Ref. [42]); —·—·—·, Griem (Ref. [1]); — — —, this paper.

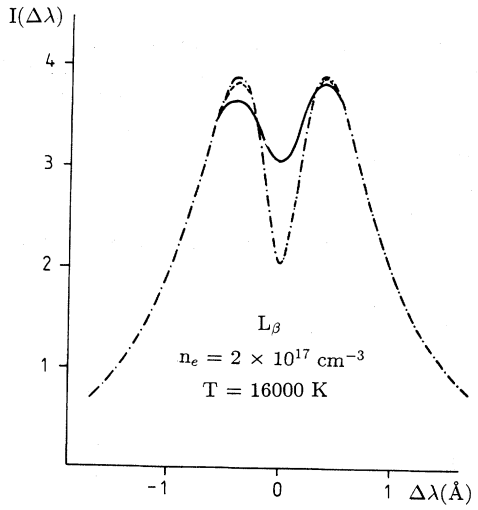

FIG. 5. Results for the L_β-line profile. ——, experiment (Ref. [43]); —·—·—·, Griem (Ref. [1]); — — —, this paper.

decreases only by about 15% [34,41] for the discussed plasma conditions. Our numerical results are included together with others in Figs. 4 and 5. They exhibit the expected behavior.

Furthermore, a comparison of measured and calculated shifts for the L_α, L_β, and H_α lines is given in Table II. In order to make a comparison, the experimental results contained in Ref. [35] have been used. In calculating the shift ($\Delta\lambda = \Delta\lambda_{el} + \Delta\lambda_{ion}$), contributions arising from the quadrupole interaction with the ions have been taken from Ref. [31]. From Table II it follows that our final results agree quite well with those of Ref. [35]. Of course, this was to be expected considering the results of the preceding discussion.

V. EFFECTS WITH INCREASING DENSITY

Up until this point, all the discussion of the theoretical and experimental results have dealt only with Stark broadening of lines within a low-density plasma. Although a many-particle interaction has been used in calculating the $\Delta n = 0$ contributions (via the Debye screening of the electron-atom interaction), its influence on the final results has remained only small.

On the other hand, the theory in Sec. II has been developed chiefly with the aim of studying the consequences of many-particle effects on the line shape. From the physical point of view, it is clear that with increasing density, the model of binary electron-atom collisions loses its applicability and, therefore, has to be replaced by a many-particle concept.

This idea has been stressed already in Ref. [49], and corresponding evaluations were carried out for L_α. However, considering small plasma parameters, only small deviations between the Debye and dynamic screening have been reported. Nevertheless, the authors claimed that with increasing values of the plasma parameter and for higher series numbers the discrepancy can increase.

Unfortunately, there are only a few experimental results for hydrogen that can be used to answer the question of whether or not one has to improve the model of Stark-broadening processes with respect to dynamic screening, and if so, at which densities one has to do so. The described situation changes to some extent if one considers other lines than those of hydrogen. Thus, for example, deviations from the general linear behavior be-

TABLE II. Comparison of the full line shifts for L_α, L_β, and H_α ($n_e = 10^{17}$ cm^{-3}).

Expt.	T (10^4 K)	$\Delta\lambda_{expt}$ (Å)	Δλ(Å) This work	Δλ(Å) Ref. [35]
Lyman α				
Ref. [42]	1.5	0.003	0.005	0.006
Lyman β				
Ref. [43]	1.6	0.005	0.013	0.013
Balmer α				
Ref. [44]	1.2	0.52	0.53	0.54
Ref. [45]	1.3	0.43		
Ref. [46]	1.3	0.57		
Ref. [47]	1.9	0.31		0.57
Ref. [48]	2.5	0.43		0.59
Ref. [50]	4.0	0.64		0.63

tween shift and electron density could be measured by different authors, and suggestions for the explanation of these findings have been given in Refs. [19] and [20]. Recently, similar results were also reported for Cs I lines at 6213 and 6355 Å [22]; the interpretation of these measurements was successful only after explicitly considering the dynamic screening effects [21].

Keeping the above in mind, the few experiments for hydrogen at higher electron densities were reconsidered, and in Ref. [50] again some deviations from the discussed linearity for the H_α shift at $n_e \approx 2\times10^{18}$ cm^{-3} and $T=70\,000$ K have been found. The discrepancy from linearity was reported to be about 30%, toward smaller values. Unfortunately, this irregularity has not been discussed by the authors and, in addition, the value of experimental errors has not been given explicitly. Further results of the H_α shift are available for $n_e \approx 10^{18}$ cm^{-3} and $T \approx 20\,000$ K [47], but they do not give rise to any deviation from linear behavior.

To compare our theory with the above experiments, the shift of H_α was calculated for the relevant plasma parameters. Once again Eq. (2.3) was used, but the approximations (3.3) and (3.4) for the imaginary part of the inverse dielectric function were avoided, using instead Eq. (3.2) within the RPA in the nondegenerate case [14]

$$\mathrm{Re}\epsilon(\mathbf{q},\omega)=1-V(q)\frac{n_e}{qk_BT}\left\{\left[\frac{\omega}{2q}+\frac{q}{2}\right]{}_1F_1\left[1,\frac{3}{2},-\frac{1}{k_BT}\left[\frac{\omega}{2q}+\frac{q}{2}\right]^2\right]-\left[\frac{\omega}{2q}-\frac{q}{2}\right]{}_1F_1\left[1,\frac{3}{2},-\frac{1}{k_BT}\left[\frac{\omega}{2q}-\frac{q}{2}\right]^2\right]\right\},$$

$$\mathrm{Im}\epsilon(\mathbf{q},\omega)=-V(q)\frac{n_e\sqrt{\pi}}{2q\sqrt{k_BT}}\left\{\exp\left[-\frac{1}{k_BT}\left[\frac{\omega}{2q}+\frac{q}{2}\right]^2\right]-\exp\left[-\frac{1}{k_BT}\left[\frac{\omega}{2q}-\frac{q}{2}\right]^2\right]\right\}, \tag{5.1}$$

where ${}_1F_1$ is the confluent hypergeometric function.

In addition, the level splitting due to the ionic microfield was taken into account, which under these conditions becomes comparable with the electron plasma frequency. Tables III and IV contain the main contributions to the shift of the upper level $(n_1,n_2,m=0,0,2)$ from $\Delta n=0$ and $\Delta n=1$ transitions, respectively. It is easy to see from Table IV that some reduction of the H_α line shift can be explained by taking into account the dynamic screening of the electron-atom interaction.

On the other hand, due to the more or less symmetrical splitting of the energy levels, the contributions of the $\Delta n=0$ transitions to the shift nearly compensate for each other. That is why the concrete approximation of screening for them has a minor influence on the final results.

With decreasing temperature, the importance of screening rises. But despite the rising importance of dynamic screening, especially for the $\Delta n=1$ contributions for $n_e=10^{18}$ cm^{-3} at $T=20\,000$ K, a linear behavior between shift and electron density results because again a compensation process takes place (compare Table IV). This is quite interesting and in complete agreement with the corresponding experimental results [47,50]. Finally, the comparison with Ref. 50 for $n_e \approx 2\times10^{18}$ cm^{-3} and $T \approx 70\,000$ K also comes out in favor of the theoretical model—although our calculated value suggests a smaller screening of only about 9%. Following our evaluations, with decreasing temperature, the screening should rise up reaching at 20 000 K about a 15% deviation from the unscreened value. A more detailed study of the expected shift lowering for H_α with increasing density will be presented elsewhere [51]. Of course, for even higher

TABLE III. Wavelength shifts of the hydrogen H_α line (only upper level 002) from $\Delta n=0$ transitions ($\Sigma_\pm$). Values in parentheses are deviations from the unscreened case.

T (10^3 K)	n_e (10^{18} cm^{-3})	ΔE (Ry)	$\Delta\lambda$ (Å) no screening	$\Delta\lambda$ (Å) dynamic screening	$\Delta\lambda$ (Å) Debye screening
		$+6.556\times10^{-4}$	+14.9	+1.5	+1.9
20	1	-6.556×10^{-4}	−13.2	+1.1	−0.5
		$\Sigma_\pm$	+1.7	+2.6 (+53%)	+1.4 (−18%)
		$+1.04\times10^{-3}$	+29.8	+2.8	+3.8
20	2	-1.04×10^{-3}	−26.4	−0.1	−1.2
		$\Sigma_\pm$	+3.4	+2.7 (−21%)	+2.6 (−24%)
		$+6.556\times10^{-4}$	+7.9	+0.8	+1.1
70	1	-6.556×10^{-4}	−7.1	0.0	−0.3
		$\Sigma_\pm$	+0.8	+0.8 (0%)	+0.8 (0%)
		$+1.04\times10^{-3}$	+15.8	+1.6	+2.2
70	2	-1.04×10^{-3}	−14.2	−0.1	−0.7
		$\Sigma_\pm$	+1.6	+1.5 (−6%)	+1.5 (−6%)

TABLE IV. Wavelength shifts of the hydrogen H_α line (only upper level 002) from $\Delta n=1$ transitions and the sum of $\Delta n=0$ and 1 contributions (0+1). Values in parentheses are deviations from the unscreened case.

T (10^3 K)	n_e (10^{18} cm^{-3})	Δn	$\Delta\lambda$ (Å) no screening	$\Delta\lambda$ (Å) dynamic screening
20	1	1	+7.1	+6.4
		(0+1)	+8.8	+9.0 (+2%)
20	2	1	+14.2	+12.3
		(0+1)	+17.6	+15.0 (−15%)
70	1	1	+7.7	+7.2
		(0+1)	+8.5	+8.0 (−6%)
70	2	1	+15.5	+14.1
		(0+1)	+17.1	+15.6 (−9%)

values of the plasma parameter the ion-electron correlation has to be treated in a more consistent manner.

VI. CONCLUSIONS

The present paper is devoted to develop a many-particle approach of a spectral-line shapes theory for the case of degenerate atomic levels. In this way, the corresponding Bethe-Salpeter equation as well as the vertex equation were reconsidered. As a result, our quantum-mechanical approach delivers contributions to the line shift from $\Delta n=0$ transitions in a natural way. Furthermore, in contrast to the case of nondegenerate atomic levels, additional vertex contributions to the shift have appeared.

The calculated H_α line profile for low electron densities agrees well with the unified theory results [32]. The disagreement with the shape of Ref. [1] is shown to be the result of the neglected degeneracy of the energy levels in dealing with the interferencelike contributions to the width there. In calculating the line shapes, the no-quenching approximation sometimes used in more basic approaches [9,12] was avoided. The same is true with the multipole expansion for the electron-atom interaction. To prove the usefulness of the weighted summing procedure introduced in Ref. [31] for the calculation of the line shift, a correct superposition of all shifted line components has been carried out.

Because of the quantum-mechanical approach used, the expressions for the line shift and width do not diverge within a Born approximation. But in order to deal with strong collisions the electron-atom scattering has to be treated by avoiding a perturbative expansion. Thus, within the Green's-function approach, a connection between the elastic phase shifts δ_l and the shift and the width of the spectral lines was used. Considering the electron scattering by the adiabatic polarization potential of the emitting atom one finds a decreasing of the strong-collision contributions compared to the result of a Born approximation.

Finally, to investigate possible higher-density effects with respect to the H_α line shift, the few available experimental findings were compared with corresponding theoretical investigations. Analyzing the results, dynamic screening effects seem to become evident with higher electron densities also for the H_α line shift. The latter would compare well with the recent experimental and theoretical findings [19,21,22]. However, further investigations have to be performed to obtain more confidence in the appearance of this many-particle effect.

APPENDIX A: SELF-ENERGY AND VERTEX CONTRIBUTIONS TO THE LINE PROFILE

Within the linear response theory, the dielectric function $\epsilon(\mathbf{k},\omega)$ describes the plasma's reaction on an external perturbing field with wave number $\mathbf{k}$ and frequency ω. Using the well-known relationship between the dielectric function, the refraction index $n(\omega)$, and the absorption coefficient $\alpha(\omega)$,

$$\lim_{k\to 0}\epsilon(\mathbf{k},\omega)=\left[n(\omega)+\frac{ic}{2\omega}\alpha(\omega)\right]^2 , \tag{A1}$$

a connection to the optical properties is given. On the other hand, the dielectric function is related to the polarization function

$$\epsilon(\mathbf{k},\omega)=1-\frac{4\pi}{k^2}\lim_{\delta\to 0}\Pi(\mathbf{k},\omega+i\delta) . \tag{A2}$$

Within the Green's-function concept Π can be investigated in a very systematic manner [14–17]. In the low-density region it is useful to introduce a cluster decompensation of the polarization function [15,19]

$$\Pi(\mathbf{k},z)=\Pi_1(\mathbf{k},z)+\Pi_2(\mathbf{k},z)+\cdots \quad (z=\omega+i\delta) , \tag{A3}$$

where Π_1 denotes the single-particle contribution. The line spectrum of an isolated atom can be found from the lowest-order contribution to $\Pi_2(\mathbf{k},z)$ given by the product of two free-particle propagators

$$G_2^0(nn',\mathbf{P},\Omega_\lambda^{ei})=\frac{-i}{\Omega_\lambda^{ei}-E_{n\mathbf{P}}^0}\delta_{nn'} , \tag{A4}$$

$\Pi_2^{(0)}(\mathbf{k},z)=$ i

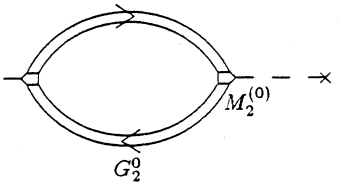

(A5)

where $M_2^{(0)}$ is the vertex function for an isolated system according to Eq. (2.5). Taking now into account the influence of the surrounding plasma, one has to replace G_2^0 by the full two-particle propagator

$G_2=$

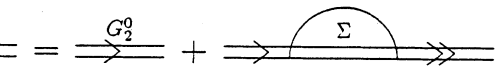

(A6)

which leads to the corrected self-energy polarization function. Σ denotes the two-particle self-energy. Using a first-order Born approximation with respect to a dynamic screened atom-electron interaction within RPA [see Eq. (2.4)],

$=iV^s(\mathbf{k},z)=\dfrac{iV(k)}{\epsilon(\mathbf{k},z)}$, (A7)

the self-energy Σ reads

$\Sigma=$

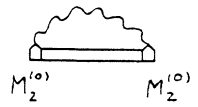

(A8)

The explicit expression for the matrix representation of Σ is given by Eq. (2.3). In order to determine the polarization function $\Pi_2(\mathbf{k},z)$, the two-particle Green's function G_2 has to be calculated. Therefore the Bethe-Salpeter equation (BSE)

$$[H^0+\mathrm{Re}\Sigma(\omega-i\delta)-(\omega\pm i\delta)]G_2(\omega\pm i\delta) \mp i\,\mathrm{Im}\Sigma(\omega-i\delta)G_2(\omega\pm i\delta)=i \quad \text{(A9)}$$

has to be solved. For the case of the nondegeneracy of the corresponding isolated atomic levels, the nondiagonal elements of $\mathrm{Im}\Sigma$ were assumed to be small compared with the diagonal ones [16,17]. Consequently, the diagonal form of G_2

$$G_2(nn',\omega\pm i\delta)=\frac{i\delta_{nn'}}{E_n^0+\langle n|\mathrm{Re}\Sigma(\omega-i\delta)|n\rangle-(\omega\pm i\delta)\mp i\langle n|\mathrm{Im}\Sigma(\omega-i\delta)|n\rangle} \quad \text{(A10)}$$

results ($\mathbf{P}=\mathbf{0}$, i.e., no Doppler broadening).

Considering emitting atoms with degenerate or close-lying energy levels, however, nondiagonal elements of the self-energy cannot be neglected further on. Therefore, the BSE (A9) has to be solved, as usual, by a matrix inversion

$$G_2(\omega\pm i\delta)=i[\mathcal{H}^{\pm}(\omega)-(\omega\pm i\delta)]^{-1} , \quad \text{(A11)}$$

with

$$\mathcal{H}^{\pm}(\omega)=H^0+\mathrm{Re}\Sigma(\omega-i\delta)\mp i\,\mathrm{Im}\Sigma(\omega-i\delta) . \quad \text{(A12)}$$

Note that for hydrogen the nondiagonal elements of the imaginary part of the plasma Hamiltonian within a spherical-wave-function representation and dipole approximation vanish for $\Delta n=0$ transitions. Finally, a straightforward calculation delivers

$$\Pi_2^{\mathrm{SE}}(\mathbf{k},z)=4\sum_{i',i'',f',f''} M_{f'i''}^{(0)*}(\mathbf{k})M_{f''i'}^{(0)}(\mathbf{k})[g_{ei}(E_i^0)-g_{ei}(E_f^0)] \times\langle i'|\langle f'|[z-H_f^0+H_i^0-\mathrm{Re}\Sigma_f+\mathrm{Re}\Sigma_i+i\,\mathrm{Im}(\Sigma_i+\Sigma_f)]^{-1}|f''\rangle|i''\rangle , \quad \text{(A13)}$$

with Eq. (2.3) and $g_{ei}(E)=[\exp\beta(E-\mu_e-\mu_i)-1]^{-1}$, where μ_e and μ_i are the chemical potentials of the electrons and ions, respectively. Besides the correction with respect to G_2, the second element in Π_2, the vertex part M_2, must be considered now on the same footing. Therefore the vertex equation

$M_2=$

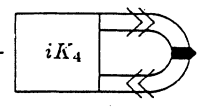

(A14)

with

$iK_4=$

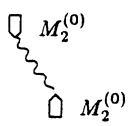

(A15)

has to be solved. For the polarization function Π_2 this results in

$$\Pi_2(\mathbf{k},z)=4\sum_{i',i'',f',f''} M^{(0)*}_{f'i''}(\mathbf{k})M^{(0)}_{f''i'}(\mathbf{k})[g_{ei}(E_i^0)-g_{ei}(E_f^0)] \times\langle i'|\langle f'|\{z-H_f^0+H_i^0-\mathrm{Re}\Sigma_f+\mathrm{Re}\Sigma_i+i[\mathrm{Im}(\Sigma_i+\Sigma_f)+\Gamma^V]\}^{-1}|f''|i''\rangle , \quad \text{(A16)}$$

where Γ^V is the vertex contribution according to (2.6) which corresponds to the well-known upper-lower cross term. The electron contribution to the line profile follows from the imaginary part of the polarization function (A16).

APPENDIX B: CONTRIBUTIONS OF STRONG COLLISIONS

An exact treatment of the electron-atom collisions has to avoid a perturbative expansion with respect to the interaction potential. If only shift and broadening of the upper energy level are taken into account, the polarization function is given by

$\Pi_2(\mathbf{k},z)=$ i 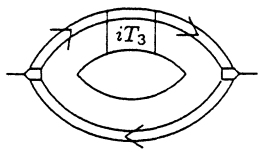

, (B1)

where T_3 is related to the three-particle propagator and is taken in the channel of the two-particle bound state and the perturbing electron. Shift and broadening of the upper level are given by the self-energy

$\Sigma_{a,e}(n\mathbf{P},n'\mathbf{P}',z)=$ 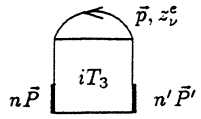

, (B2)

where T_3 follows from the solution of the three-particle problem containing elastic and inelastic (excitation) processes. Considering only elastic electron-atom scattering ($n=n'$), the shift and broadening of the energy level follow from [28]

$$\Delta_{n,\mathbf{P}}+i\Gamma_{n,\mathbf{P}}=\langle n|\Sigma_{a,e}(\mathbf{P},E_n^0-i0)|n\rangle . \quad \text{(B3)}$$

According to Eq. (B3) the self-energy leads to

$$\Sigma_{a,e}(n\mathbf{P},z)=\frac{1}{(2\pi)^3}\int d\mathbf{p}\, T_{a,e}(n\mathbf{P}pn,\mathbf{P}p,z +E_e(p))f_e(E_p) , \quad \text{(B4)}$$

with f_e the Fermi distribution function. In order to find a relationship between phase shifts for an elastic-scattering process and the upper-level shift and width, the three-particle T matrix T_3 will be written in terms of the phase shifts [52]

$$T_{a,e}(\mathbf{p}-\mathbf{p}')=-\frac{2\pi}{m_e}\sum_{l=0}^{\infty}(2l+1)P_l(\cos[\sphericalangle(\mathbf{p},\mathbf{p}')]) \times\frac{1}{p}e^{i\delta_l(E_p)}\sin\delta_l(E_p) . \quad \text{(B5)}$$

Note that shift and broadening result from forward scattering ($\mathbf{p}=\mathbf{p}'$) [24].

Thus the problem is transformed into the calculation of phase shifts for which further approximations are necessary. For simplicity, a partial summation of the perturbative expansion has been used which yields the polarization potential [28]

$$V^P(n\mathbf{P}p,n\mathbf{P}+\mathbf{q}p-\mathbf{q}) =\frac{1}{e^2}\sum_{n''(\neq n)}\frac{1}{(2\pi)^3}\int d\mathbf{q}'V(\mathbf{q}')V(\mathbf{q}-\mathbf{q}') \times\frac{M_{nn''}(\mathbf{q}')M_{n''n}(\mathbf{q}-\mathbf{q}')}{E_{n\mathbf{P}}+E_{\mathbf{p}}-E_{n''\mathbf{P}+\mathbf{q}'}-E_{\mathbf{p}-\mathbf{q}'}} . \quad \text{(B6)}$$

For the L_α line considered here one may neglect both shift and broadening of the lower energy level as well as vertex corrections. In order to evaluate the upper-level shift of L_α, in a first approximation only the shift of the dominant L_α component corresponding to the transition $001\rightarrow 000$ (in parabolic quantum numbers) has been taken into account. Treating this component as isolated, the kinetic energies of electron and atom may be neglected in Eq. (B6), and an adiabatic approximation for the polarization potential may be used [29]. For the present aim, this polarization potential can be given by the interpolation formula [30]

$$V^P(R,n)\approx-\frac{e^2}{2}\frac{\alpha_n}{(R^2+r_0^2)^2} . \quad \text{(B7)}$$

Here α_n denotes the dipole polarizability of the atom in the internal state n

$$\alpha_n=-2e^2\sum_{n''(\neq n)}|d_{nn''}|^2(E_n-E_{n''})^{-1} , \quad \text{(B8)}$$

with

$$d_{nn''}=\int d\mathbf{r}\,\Psi_n^*(\mathbf{r})\mathbf{r}\Psi_{n''}(\mathbf{r})\ . \tag{B9}$$

The cutoff radius r_0 is determined by

$$r_0=\left[\frac{(e^2/2)|\alpha_n|}{|V^P(0,n)|}\right]^{1/4}, \tag{B10}$$

with

$$V^P(R=0,n)=e^4\sum_{n''\,(\neq n)}\frac{1}{E_n-E_{n''}}\left|\int d\mathbf{r}\,\Psi_n^*(\mathbf{r})\frac{1}{r}\Psi_{n''}(\mathbf{r})\right|^2. \tag{B11}$$

Phase-shift calculations have been performed for this potential using $\alpha_{001}=156a_B$ (see Ref. [26]) and $r_0=4.998a_B$, where a_B denotes the Bohrs radius.

[1] H. R. Griem, *Plasma Spectroscopy* (McGraw-Hill, New York, 1964); *Spectral Line Broadening in Plasmas* (Academic, New York, 1974).
[2] D. M. Ross, Ann. Phys. (N.Y.) **36**, 458 (1966).
[3] H. R. Zaidi, Phys. Rev. **173**, 123 (1968); **173**, 132 (1968).
[4] L. Klein, J. Quant. Spectrosc. Radiat. Transfer **9**, 199 (1969).
[5] M. W. C. Dharma-wardana, F. Grimaldi, A. Lecourt, and J. L. Pellisier, Phys. Rev. A **21**, 379 (1980).
[6] B. Bezzerides, J. Quant. Spectrosc. Radiat. Transfer **7**, 353 (1967).
[7] B. Bezzerides, Phys. Rev. **159**, 3 (1967).
[8] D. Voslamber, Z. Naturforsch. **24A**, 1458 (1969); **27A**, 1783 (1972); Phys. Lett. **40A**, 266 (1972).
[9] C. R. Vidal, J. Cooper, and E. W. Smith, J. Quant. Spectrosc. Radiat. Transfer **10**, 1011 (1970); **11**, 263 (1971); Astrophys. J. Suppl. **25**, 37 (1973).
[10] J. W. Dufty and D. B. Boercker, J. Quant. Spectrosc. Radiat. Transfer **16**, 1065 (1976).
[11] C. A. Iglesias, J. Quant. Spectrosc. Radiat. Transfer **30**, 55 (1983); Phys. Rev. A **29**, 1366 (1984).
[12] D. B. Boercker and C. A. Iglesias, Phys. Rev. A **30**, 2771 (1984).
[13] W. Ebeling, W. D. Kraeft, and D. Kremp, *Theory of Bound States and Ionization Equilibrium in Plasmas and Solids,* Ergebnisse der Plasmaphysik und Gaselektronik Vol. 5 (Akademie-Verlag, Berlin, 1976).
[14] W. D. Kraeft, D. Kremp, W. Ebeling, and G. Röpke, *Quantum Statistics of Charged Particle Systems* (Akademie-Verlag, Berlin, 1986).
[15] G. Röpke and R. Der, Phys. Status Solidi B **92**, 501 (1979).
[16] G. Röpke, T. Seifert, and K. Kilimann, Ann. Phys. (Leipzig) **38**, 381 (1981).
[17] L. Hitzschke, G. Röpke, T. Seifert, and R. Zimmermann, J. Phys. B **19**, 2443 (1986).
[18] L. Hitzschke and G. Röpke, Phys. Rev. A **37**, 4991 (1988).
[19] G. Röpke and L. Hitzschke, in *Proceedings of the Ninth International Conference on Spectral Line Shapes,* edited by J. Szudy (Ossolineum, Wrocław, 1989), p. 49.
[20] L. Hitzschke, Ph.D. thesis, 1987, Humboldt Universität Berlin.
[21] L. Hitzschke, in *Nineteenth International Conference on Phenomena in Ionized Gases,* Contributed Papers, edited by J. M Lebet (University of Belgrade, Belgrade, 1989), p. 348.
[22] R. Radtke and M. Kettlitz, in *Nineteenth International Conference on Phenomena in Ionized Gases* (Ref. [21]), p. 350.
[23] C. A. Iglesias and J. W. Dufty, in *Spectral Line Shapes,* edited by K. Burnett (de Gruyter, Berlin, 1983), p. 55.
[24] M. Baranger, Phys. Rev. **111**, 481 (1958); **111**, 494 (1958); **112**, 855 (1959).
[25] C. F. Hooper, Phys. Rev. **165**, 215 (1968).
[26] H. A. Bethe and E. E. Salpeter, *Quantum Mechanics of One- and Two-Electron Atoms* (Springer-Verlag, Berlin, 1957).
[27] A. Tsuji and H. Narumi, Prog. Theor. Phys. **44**, 1557 (1970).
[28] R. Redmer, G. Röpke, and R. Zimmermann, J. Phys. B **20**, 4069 (1987).
[29] P. M. Stone and J. R. Reitz, Phys. Rev. **131**, 2101 (1963).
[30] R. A. Buckingham, Proc. R. Soc. London Ser. A **160**, 94 (1937).
[31] H. R. Griem, Phys. Rev. A **28**, 1596 (1983).
[32] L. J. Roszman, Phys. Rev. Lett. **34**, 785 (1975).
[33] D. H. Oza, R. L. Greene, and D. E. Kelleher, Phys. Rev. A **37**, 531 (1988).
[34] M. A. Gigosos and V. Cardeñoso, J. Phys. B **20**, 6005 (1987).
[35] H. R. Griem, Phys. Rev. A **38**, 2943 (1988).
[36] W. L. Wiese, D. E. Kelleher, and V. Helbig, Phys. Rev. A **11**, 1854 (1975).
[37] J. Seidel, Z. Naturforsch. **32A**, 1207 (1977).
[38] M. A. Gigosos and V. Cardeñoso, Ann. Phys. (Paris) **11**, 185 (1986).
[39] R. Stamm, E. W. Smith, and B. Talin, Phys. Rev. A **30**, 2039 (1984).
[40] K. Grützmacher and B. Wende (unpublished).
[41] D. H. Oza and R. L. Greene, J. Phys. B **21**, L5 (1988).
[42] K. Grützmacher and B. Wende, Phys. Rev. A **16**, 243 (1977).
[43] K. Grützmacher and B. Wende, Phys. Rev. A **18**, 2140 (1978).
[44] J. Halenka, in *Proceedings of the Seventeenth International Conference on Phenomena in Ionized Gases,* edited by J. S. Bakes and Z. Sörley (Hungarian Academy of Science, Budapest, 1985), p. 993.
[45] D. E. Kelleher, N. Konjević, and W. L. Wiese, Phys. Rev. A **20**, 1195 (1979).
[46] W. L. Wiese, D. E. Kelleher, and D. R. Paquette, Phys. Rev. A **6**, 1132 (1972).
[47] Y. Vitel, J. Phys. B **20**, 2327 (1987).
[48] M. K. Salakhov, E. V. Sarandaev, R. Z. Latipov, and I. S. Fishman, Opt. Spektrosk. **60**, 431 (1986) [Opt. Spectrosc. (USSR) **60**, 264 (1986)].
[49] T. W. Hussey, J. W. Dufty, and C. F. Hooper, Phys. Rev. A **16**, 1248 (1977).
[50] K. H. Finken, R. Buchwald, G. Bertschinger, and H.-J. Kunze, Phys. Rev. A **21**, 200 (1980).
[51] S. Günter and L. Hitzschke (unpublished).
[52] A. Messiah, *Quantum Mechanics* (North-Holland, Amsterdam, 1965), Vol. 1.